# Investigation on the Behavior of Posttensioned Energy Dissipation Connections under Fire Loading

**Azin Al kajbaf[1]\*, Nader Fanaie[2]**

1. M.Sc. Student, Civil Engineering Department, K.N. Toosi University of Technology, Tehran, Iran, aalkajbaf@mail.kntu.ac.ir
2. Assistant Professor, Civil Engineering Department, K.N. Toosi University of Technology, Tehran, Iran, fanaie@kntu.ac.ir

## Abstract

Posttensioned energy dissipation (PTED) connections are systems developed to be used in structures which are located in seismic prone areas. These structural systems reduce the earthquake damage by removing the residual drift and dissipating the seismic energy. Following an earthquake, one of the most probable scenarios is a fire event. Therefore, understanding the behavior of PTED connections, which their primary application is in seismic areas, is of significant importance. This paper presents an analytical study on the behavior of a PTED connection with bolted top-and-seat angles subjected to the fire loading. Finite element model of a PTED connection is developed and verified based on experimental results. Another experimental study is selected which includes a beam-to-column subassembly with web cleat joints subjected to the fire loading. This connection is also modeled using finite element analysis and is validated using experimental results. Since no experimental data is available for PTED connections under fire condition, this verified model is employed to make sure that the behavior of an angle connection at elevated temperature is modeled accurately. Afterwards, PTED connection model is subjected to the fire loading. The analysis is conducted assuming three cases of PTED connection with unprotected strands, with protected strands and without strands. Temperature-rotation curves are derived and compared. The results show that the behavior of a PTED connection with unprotected strands is not considerably different than that of a typical semi-rigid connection subjected to the fire. However, using fire protection coating for strands significantly reduces the connection rotation and therefore prevents the structural collapse.

**Key words:** finite element modeling, fire loading, posttensioned strands, PTED connection

## 1. Introduction

The idea of new moment resisting frames (MRFs) emerged after the 1994 Northridge earthquake. Several steel MRFs failed during this destructive phenomenon which was mostly due to the brittle fracture in the beam-to-column connections [1]. A typical connection in a welded MRF that was widely used in seismic areas before the Northridge earthquake contained a shear-tab bolted to the beam web and groove weld between the beam and the column flange [2]. Due to the ductility of steel, these frames were expected to experience inelastic deformation and therefore dissipate seismic energy.

Inelastic deformation leads to formation of plastic hinges which are mostly anticipated to be formed in the beams. However, these plastic hinges did not form during the earthquake which resulted in extensive damage in the connections. Among many factors that induced the damage, the fracture that initiated from the field weld of the beam bottom flange was the major reason [3]. After the Northridge earthquake, efforts were made to develop an enhanced

MRF which does not experience premature weld failure, including connections retrofitted with locally reduced beam sections (RBS) [4] and connections with cover plates [5].

PTED connection was alternatively suggested to be utilized in MRFs. These connections contain high strength posttensioned (PT) elements like bars or strands and energy dissipater (ED) devices. Figure 1(a) demonstrates an exterior PTED connection with top-and-seat angles. PT strands are placed at each side of the beam web and pass through the column flanges. Following an earthquake, a gap is opened in the beam to column face. Due to the posttensioning force in the strands, they are willing to bring the frame back to its initial position which gives the structure the ability to self-center (SC) and results in minimizing the residual deformation. During cyclic displacement of the frame, angles undergo plastic deformation and therefore dissipate the input seismic energy. Figure 1(b) plots moment-rotation $(M - \theta_r)$ response of a typical PTED connection, in which $\theta_r$ is relative rotation between the beam and the column. Before gap opening, the stiffness of the connection is equal to that of a welded connection. Nevertheless, upon gap opening it is associated with stiffness of the angles and elastic stiffness of the strands. During loading of the frame, the angles yield and form plastic hinges. Throughout unloading the angles dissipate energy until the strands bring the connection back to its initial position and the gap is closed ($\theta_r = 0$) [6].
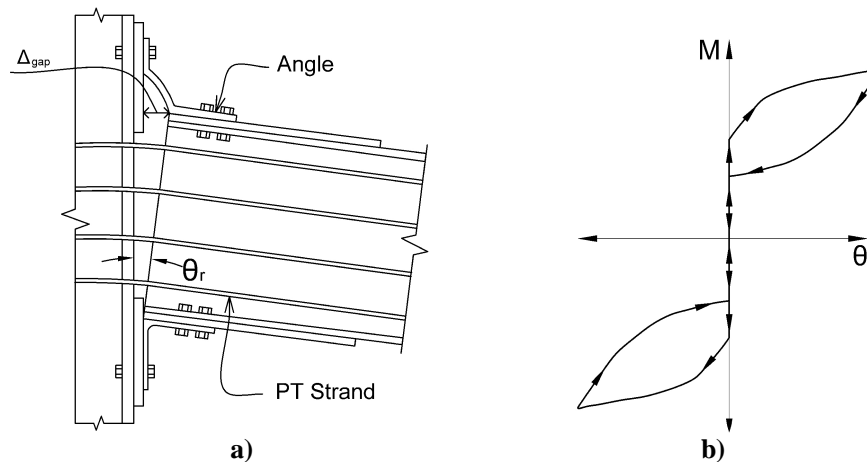


**Figure 1: a) Decompressed PTED connection [6], b) Moment-rotation response of a PTED connection [6]**

In PTED connections, damage is restricted to ED devises which can be easily replaced and the structural components remain elastic during the entire seismic loading.

The first PTED connection was designed and experimentally tested by Ricles *et al.* (2001) [7] which had high strength strands and top-and-seat angles as ED device. Ricles *et al.* [8] and Garlock *et al.* [6, 9] carried out experimental studies to investigate the behavior of PTED beam-to-column sub-assemblies with top-and-seat angles under cyclic loading and their effective factors such as angle parameters and initial posttensioning force of strands. Other than the angles, researches have suggested different elements to be used as ED device such as bars, reduced flange plates and hourglass shaped cylindrical pins [1, 10, 11].

The response of a steel structure subjected to the fire has been the matter of interest for researchers in recent decades. The behavior of joints in particular, strongly influences the overall behavior of the structure and should be taken into account in global analysis. In ambient temperature the connections are either considered as rigid or pinned in order to simplify the analysis [12]. However, due to the complicated situation in a fire condition these

assumptions cannot be used. The behavior of a connection should be properly determined, since it  has a significant effect on the progressive collapse of a structure caused by a fire event [13]. In this regard, numerous experimental and analytical studies have been conducted. Yu *et al.* (2008) [14] performed an experimental and analytical study to investigate the robustness of a web-cleat connection under fire. The results demonstrated that this connection has great ductility and experiences different modes with respect to its temperature. Wang *et al.* (2011) [15] conducted an experimental study on the behavior of various types of steel connections including web cleat, flush endplate, extended endplate, flexible endplate and fin endplate under fire. Failure modes and axial force of the connection at elevated temperature were investigated. Experimental and numerical studies were carried out by Qiang *et al.* (2014) [16, 17] regarding the behavior of high strength endplate connection subjected to steady state fire condition. The results were compared to that of endplate connection made of mild steel. It was found that a high strength endplate with sufficient thickness improves the rotation capacity of the connection.

Despite the fact that several studies have been done on the different types of PTED connections during the last decade, there is still no experimental test concerning the behavior of these connections under fire condition. Nonetheless, there is a great possibility for fire to occur during or post an earthquake. Therefore, it is important to study the response of PTED connections subjected to fire. In this regard, finite element (FE) analysis can be employed which has been proved to be a suitable method that is able to confirm the experimental results and moreover, provides the possibility to further investigate and capture the behavior of experimental specimens from different aspects at much lower cost.

The main objective of this paper is to study the behavior of posttensioned connections under fire condition and to investigate the effect of PT strands on the connection rotation at elevated temperatures. FE model of a PTED connection specimen with top-and-seat angles that was tested by Garlock *et al.* (2005) [6] is developed using ABAQUS software [18]. The behavior of the specimen is verified based on experimental results. Then, another experimental study conducted by Wang *et al.* (2011) [15] is selected which contains testing of a beam-to-column subassembly with web cleat joint under fire. This connection is modeled using FE analysis and validated against experimental results. This connection is simulated to confirm the precision of modeling the behavior of an angle connection at elevated temperatures. Eventually, PTED connection model is subjected to the fire loading. Three models are developed including PTED connection with unprotected strands, with fire protection coating for the strands and without strands. Temperatures-rotation curves of each model are derived and compared to each other.

## 2. Development of the finite element model of a PTED connection
### 2-1- Modeling procedure

3D model is developed using non-linear FE analysis program (ABAQUS) to simulate the behavior of an interior PTED connection studied by Garlock *et al.* (2005) [6, 18]. In their study, six PTED beam-to-column specimens with high strength strands and top-and-seat angles were experimentally tested under cyclic loading. Specimens were almost the same with differences in number of strands, length of reinforcing plate and total initial posttensioning force, so that different limit states could be reached. For this study, specimen 36s-20-P is chosen and modeled. This specimen has 36 strands, reinforcing plate with length 1372 *mm* and total initial posttensioning force of 3194 *kN* . The test setup in Garlock *et al.* (2005) [6] experiment is shown in Figure 2(a).
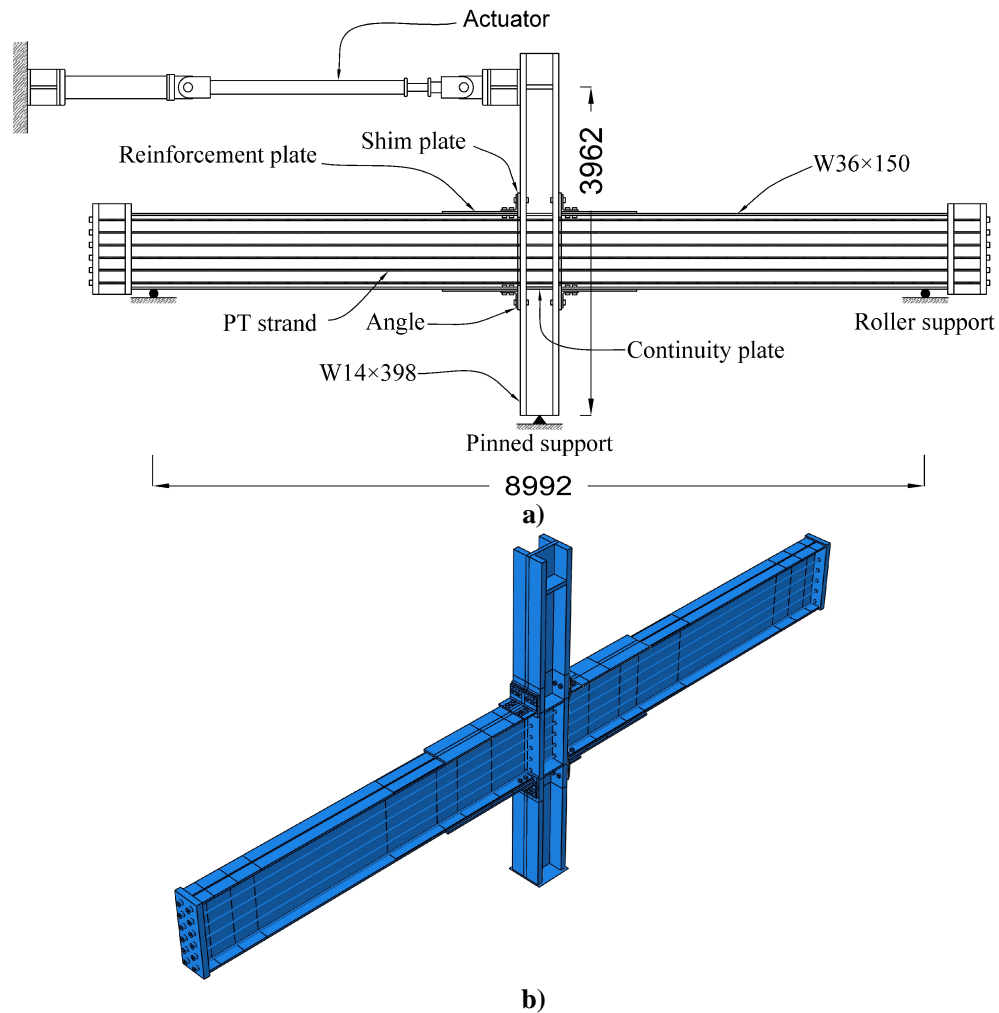
**Figure 2: a) Test setup in Garlock *et al.* (2005) experiment [6], b) Test setup in FE model**

Span length from one vertical support to the other is $8992\,mm$ and the column height is $3962\,mm$ . Specimen is made of W14×398 column and W36×150 beams. The PT strands are placed at both side of the beam web in six evenly spaced rows in groups of three. Each strand has area of 140 $mm^2$ and passes through 44 $mm$ holes drilled in the column flange. L8×8×3/4 angles are positioned on top and bottom flanges of the beams. These angles are connected to the column and beam through one row of four and two rows of two A490 bolts respectively. Shim plates with dimensions of 292×406×32 $mm$ are welded to the column flanges in order to compensate the reduced net section of the column flange due to the presence of holes. Reinforcing plates with dimension of 356×25 $mm$ are shop welded to the beam flanges so that they could prevent it from local buckling. In order to keep the panel zone elastic, one doubler plate with 19 $mm$ thickness and two continuity plates with 25 $mm$ thickness are welded to the web and flanges of the column.

The FE modeling reproduced the actual geometry of the test setup proposed in the experimental study with slight differences. In FE modeling, three strands which were placed together and passed through one hole in the test setup are not simulated separately. Instead of three strands with areas of $140\,mm^2$ for each one, one strand with area of 420 $mm^2$ is modeled. Also short anchor columns are not simulated. Alternatively two plates are placed at

the end of the beams and strands are anchored against them. These changes simplify the analysis and do not affect the results. All of the members were modeled with deformable solid elements.

Bolts and strands are made of ASTM A490 and A416 respectively. Other members are made of ASTM A572 Grade 50 steel. Table 1 lists the material properties that were obtained for different members through material test by Garlock *et al.* (2005) [6]. The PT strands have Young's modulus and tensile capacity of $199 GPa$ and $266 kN$ respectively. Young's modulus of other members is taken as $200 GPa$. Density and Poisson's ratio ( ) of all components are equal to 7850 $kg / m^3$ and 0.3 respectively.

**Table 1: Material properties (Garlock *et al.* (2005) [6])**

| Item | $\dagger_y (MPa)$ | $\dagger_u (MPa)$ |
|---|---|---|
| Beam flange | 362 | 498 |
| Beam web | 414 | 527 |
| Reinforcing plates | 397 | 574 |
| Column flange | 356 | 499 |
| Column web | 345 | 545 |
| Angles | 383 | 523 |
| PT stands | 1620 | 1900 |

Contact behavior between welded parts is defined using tie constraint. Interaction between other components is defined using general contact algorithm. Tangential and normal behavior is assigned to contacting surfaces. Tangential behavior between bolt shank and bolt hole and also between strand and strand hole is assigned as frictionless. Tangential behavior between other surfaces is defined using penalty method. Friction coefficient is taken as 0.35 based on AISC provisions (2005) [19]. Normal behavior is considered hard contact to prevent two adjacent surfaces from penetrating.

Roller boundary condition is considered for each beam 4496mm distant from column centerline (vertical displacement is zero). Column has pin support at the base which restricts the displacement in any direction and allows it to rotate freely. In experimental study cyclic loading was applied by two actuators at top of the column flange. In the experiment the loading cycles included "six cycles at u=0.375, 0.50, and 0.75%, four cycles at u=1.0%, and two cycles at u=1.5, 2, 3, and 4% drift" [6]. In the FE modeling only one cycle of 4% drift is applied to the model to reduce the computational time. Story drifts is applied as displacement. Strands and bolts are pre-tensioned in accordance with the experimental study [6].

ABAQUS Explicit procedure is used for the analysis [18]. This non-linear analysis method is appropriate for models with great number of contact elements which undergo large deformations and material degradation [18]. Since the current FE model has numerous contact surfaces and experiences local buckling, ABAQUS Explicit is selected as the analysis method [18].

The members are meshed by 3D hexahedral element (C3D8R) with reduced integration and hourglass control [18]. A mesh study was conducted to find the appropriate mesh size that gives enough accuracy to the analytical results. Finer meshes are defined for panel zone and angles. Figure 3 shows meshing details of the panel zone.
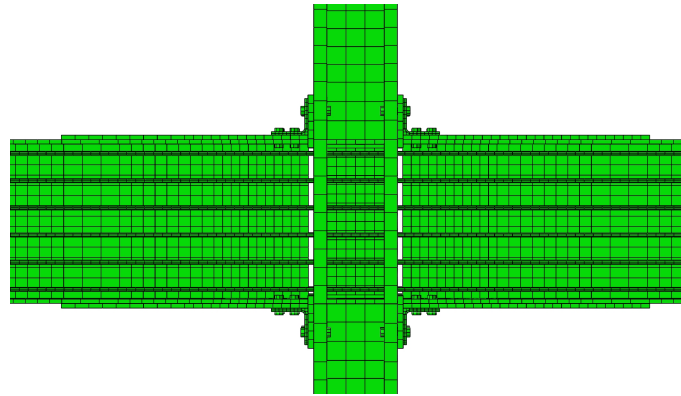
**Figure 3: Meshing details of the panel zone in specimen 36s-20-P**

## 2-2- Finite element results of PTED connection

The FE model of specimen 36s-20-P experimentally studied by Garlock *et al.* (2005) [6] was developed. Figure 4 compares lateral load-displacement curve of FE model and experimental specimen. Lateral load and displacement are calculated at the point where the load is applied on top of the column flange. It can be seen that the FE result is in good correlation with the experimental one.
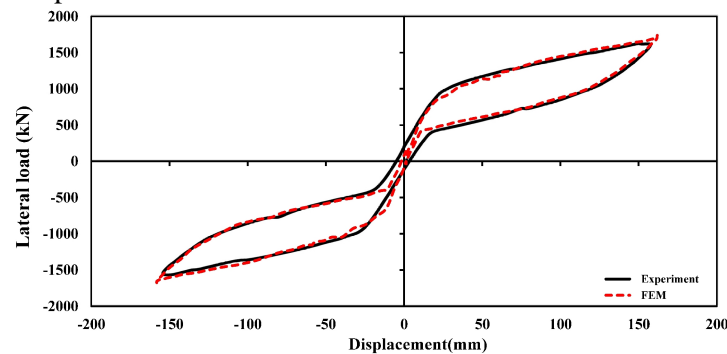


**Figure 4: Comparison of lateral load-displacement response in experimental and FE model of specimen 36s-20-P [6]**
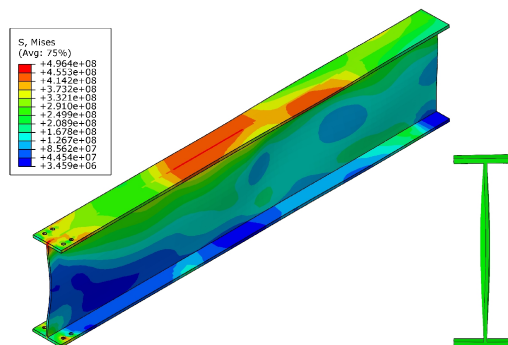


**Figure 5: Deformed shape and von Mises stress distributuion in specimen 36s-20-P at 4% story drift**

In the experimental study, specimen 36s-20-P was subjected to up to 4% story drift and was expected to experience the limit state of angle fracture. Nevertheless, after two and half cycles of 4% story drift, the test was terminated due to the local buckling in beam web while

the angles were left undamaged. Figure 5 depicts the beam web buckling at 4% story drift in FE modeling and von Mises stress distribution. In the experimental study, beam web buckled which had a single wave with amplitude of 6.35 mm. In the FE model the single wave in beam web has amplitude of 9 mm.

## 3. Development of finite element model of the connection with web cleat joint

### 3-1- Modeling procedure

A beam-to-column subassembly with web cleat joint is modeled using FE analysis [18]. This specimen amongst other beam-to-column subassemblies with various joints, containing flush endplate, extended endplate, flexible endplate and fin endplate, was experimentally tested under fire condition by Wang *et al.* (2011) [15]. Two different column sizes were employed to examine the effect of axial restraining force in the beams. The structural fire performance such as connection failure modes and deflection of the beam middle span were investigated for the specimens. It was determined that the web cleat joint have the best behavior between the other specimens. Figure 6(a) illustrates the test setup in Wang *et al.* (2011) [15] experiment. As it is shown, the test setup consists of one beam and two columns with similar beam-to-column joints. Specimen with test ID 4 is selected for FE modeling. It is consists of UC254×254×72 columns and UB178×102×9 beam. Angles with dimensions of 90×150×10 *mm* and width of 130 *mm* are placed at both sides of the beam web. One row of two and two rows of two Grade 8.8 M20 bolts connects the angles to the column flange and beam web, respectively. Due to the symmetrical geometry, only half of the test setup is modeled. Figure 6(b) shows 3D view of the FE model. All of the components are modeled using 3D deformable solid elements.
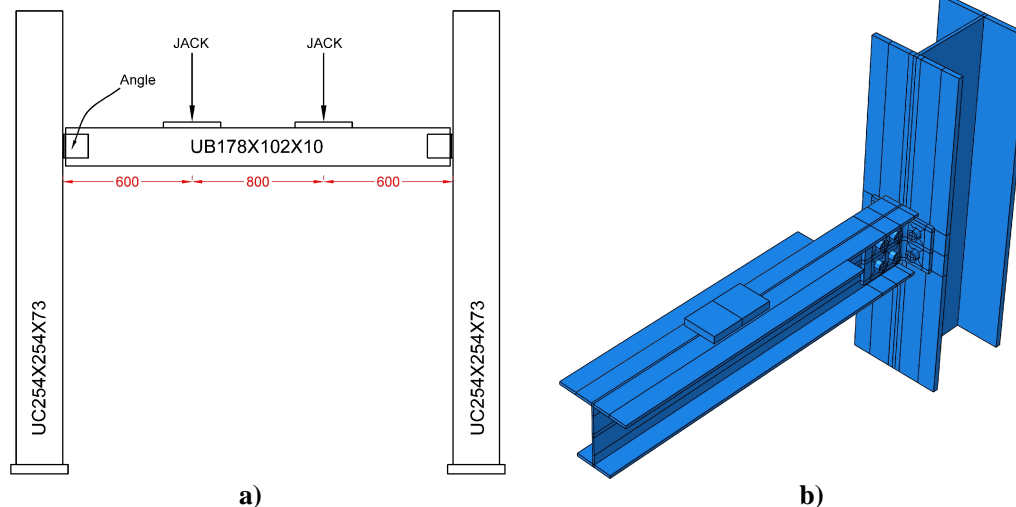


|  a) | b) |

**Figure 6: a) Test setup in Wang *et al.* (2011) [15] experiment, b) Test setup in the FE modeling**

Columns and web cleats are made of Grade S355 and Grade S275 steel, respectively. Material properties of members were obtained through tensile coupon test at ambient temperature [13]. Modulus of elasticity, yield strength, maximum strength and ultimate strain are listed in table 2. The modulus of elasticity and nominal yield strength of bolts were taken as $210000\,MPa$ and $640\,MPa$ respectively in accordance with assumption made in numerical study by Dai *et al.* (2010) [13]. Density and Poisson's ratio ( ) for all of the elements are defined as 7850 $kg\,/\,m^3$ and 0.3, respectively. For material properties at elevated temperatures,

reduction factors of EC3 (EN1993-1-2) [20] for carbon steel are used. Figure 7 plots reduction factor for stress-strain relationship of steel at elevated temperatures.

**Table 2: Material properties (Dai *et al.* (2010) [13])**

| Member | Modulus of elasticity ($MPa$) | Yield strength ($MPa$) | Maximum strength ($MPa$) | Ultimate strength ($MPa$) |
|---|---|---|---|---|
| Beam | 226580 | 344 | 514 | 28.2 |
| Column | 200000 | 390 | 553 | 25 |
| Web cleat | 228170 | 342 | 493 | 32.6 |
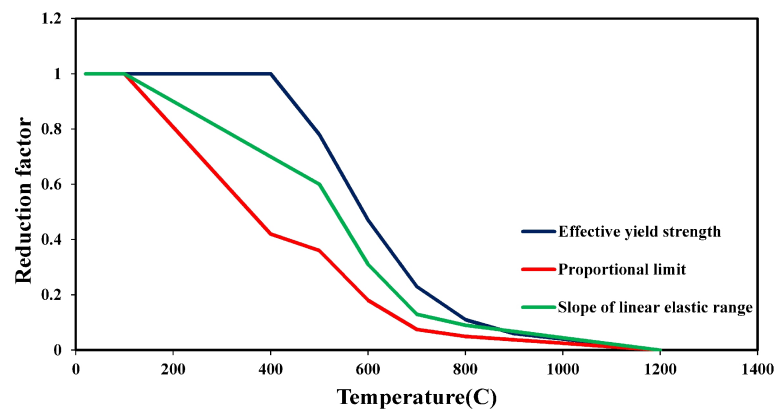


**Figure 7: Reduction factors for stress-strain relationship of carbon steel at elevated temperatures [20].**

Welded parts are modeled using tie constraint. Interaction between contacting surfaces is defined using general contact algorithm.

In accordance with the experimental test setup, pin support condition is assigned to the bottom of the column. The displacement of the top of the column is restrained in two directions, but it is free to move in its axial direction. The movement of the beam along its axial direction is also restricted due to the symmetrical condition applied in the FE modeling. In the experiment a steel truss was bolted to the beam top flange so that the effect of concrete slab on restraining the lateral movement of the beam could be simulated. However, in numerical modeling by Dai *et al.* (2010) [13] this truss was replaced with two 750×50×8 *mm* plates that were designed to produce the same lateral restraining force for the beam. As shown in figure 6(a) in the experiment two hydraulic jacks, each applied 40 *kN* loads to the beam at ambient temperature were maintained through the entire time of the heating phase. In the FE modeling the 40 *kN* load is applied with a loading plate tied to the beam top flange as shown in figure 6(b) in an individual step. In the next step the temperature is increased while keeping the 40 *kN* load. As mentioned in the experimental study, all of the members are subjected to the heating in the furnace except for the beam top flange and the truss which were protected to account for the effect of concrete slab [15]. Same condition is considered in the FE model.

ABAQUS Explicit procedure is employed for the analysis. All of the elements are meshed using 3D hexahedral elements (C3D8T and C3D8R) with reduced integration and hourglass control. A mesh study was done to find the suitable mesh size. Figure 8 shows the meshing details of web cleat.
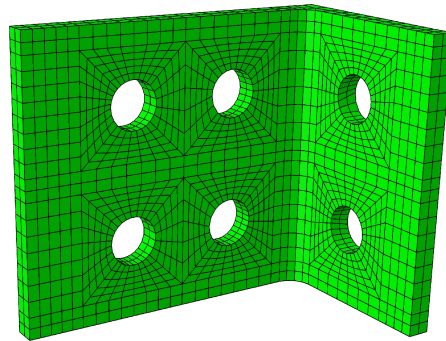
**Figure 8: Meshing details of web cleat in specimen 4**

### 3-2- Finite element result of the connection with web cleat joint

To evaluate the precision of  modeling the behavior of angle connection at elevated temperatures, the FE model of specimen 4 in experimental study of Wang *et al.* (2011) [15] was developed. In figure 9 the beam deflection-temperature curve obtained from FE modeling is compared to those from experimental test by Wang *et al.* (2011) [15] and FE simulation by Dai *et al.* (2010) [13]. It can be seen that FE result is in good agreement with corresponding experimental one. According to Wang *et al*. (2011) [15] the differences in FE and experimental result might be due to the heating non-uniformities that were faced in test.

The deformed shape of the FE model of specimen 4 is demonstrated in figure 10. According to the deformed shape of the experimental specimen presented in Wang *et al.* (2011) [15] study, FE modeling could properly simulate the behavior of the connection with web cleat joint at elevated temperatures.
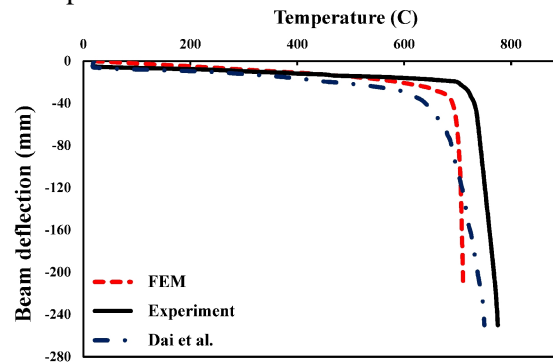


**Figure 9: Comparison of beam deflection-temperature curves in experimental and FE model of specimen 4 [13, 15]**
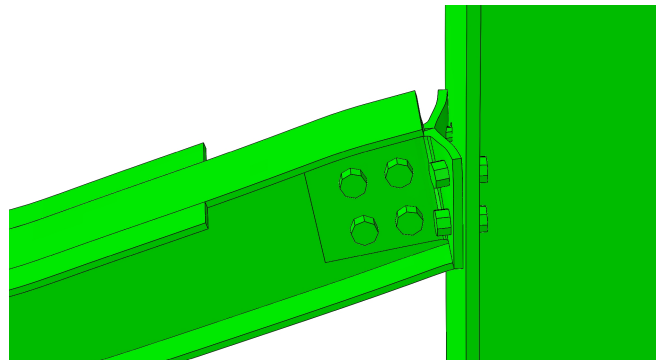


**Figure 10: Deformed shape of specimen 4**

## 4. Finite element model of PTED connection under fire loading
### 4-1- Modeling procedure
In order to simulate the behavior of PTED connection under fire loading, the FE model of specimen 36s-20-P subjected to cyclic loading should be modified. Reduction factors of EC3 (EN1993-1-2) (figure 7) are employed to model the behavior of material at elevated temperatures. Few changes are made to the test setup and boundary conditions. Instead of applying cyclic loading at top of the column flange, constant loads are applied to each beam at the loading points as indicated in figure 11. Beam supports are eliminated and column support is changed to fixed support.
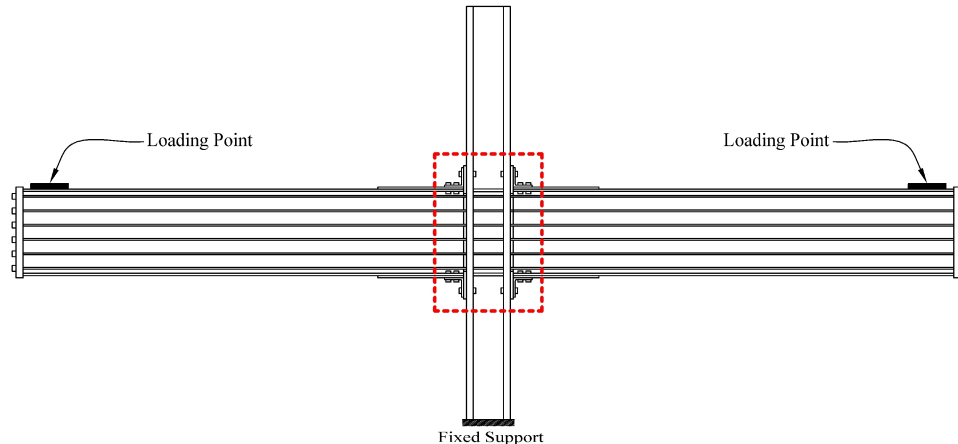


**Figure 11: Test setup of PTED connection subjected to fire in FE modeling**

ABAQUS Explicit procedure is used for the analysis. The analysis is conducted in three steps. In the first step, strands and bolts are pre-tensioned. In the second step, the constant loads are applied to the beams. In the third step, the connection zone as shown in figure 11 is subjected to the fire, while constant loads are kept on the beams. Constant loads are considered as half of the plastic moment capacity of the connection. Mesh elements in the fire zone are changed to C3D8T.

In order to accurately evaluate the effects of strands in the PTED connection, three cases are considered. In the first case, strands are present and part of them which is located in the fire zone is subjected to the fire. In the second case, strands are present but they are protected against fire with fire protection coating. In the third case, strands are eliminated from the FE model.

### 4-1- Finite element results of PTED connection subjected to the fire loading
To investigate the effects of strands on the behavior of the PTED connection, three models were developed as discussed in previous section. The temperature-rotation curves of these specimens are compared in figure 12. The rotation of the connection can be obtained as follows[21]:

$$\{ =\tan^{-1}(u/L) \tag{1}$$

Where $u$ is the vertical displacement of a point along the beam and $L$ is the distance from the connection centerline to the point where the vertical displacement is measured.

As it is shown in figure 12, up to 300 degrees Celsius, all of the models have the same initial stiffness which is due to the inconsiderable changes in the steel properties till this temperature. Although up to 600 degrees Celsius, the temperature-rotation curve of the model with protected strands overlays on that of the model with unprotected strands, it can be seen

that the model with protected strands does not have a visible yielding plateau. Comparing the curves of the models with unprotected strands and without strands determines that both models have similar connection rotations.
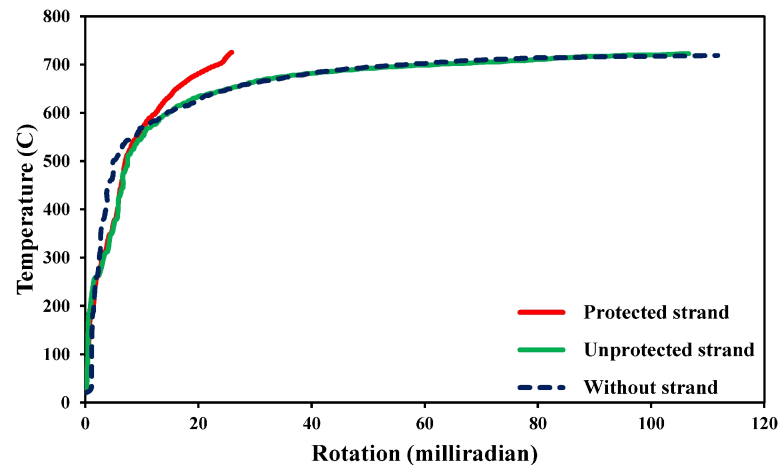


**Figure 12: Comparison of temperature-rotation curves of PTED connection subjected to fire loading in three cases of, with unprotected strands, with protected strands and without strands**

Figure 13 shows the FE model without strands at 715 degrees Celsius. It can be seen that eliminating the strands resulted in significant connection rotation and plastic deformation in the angles.
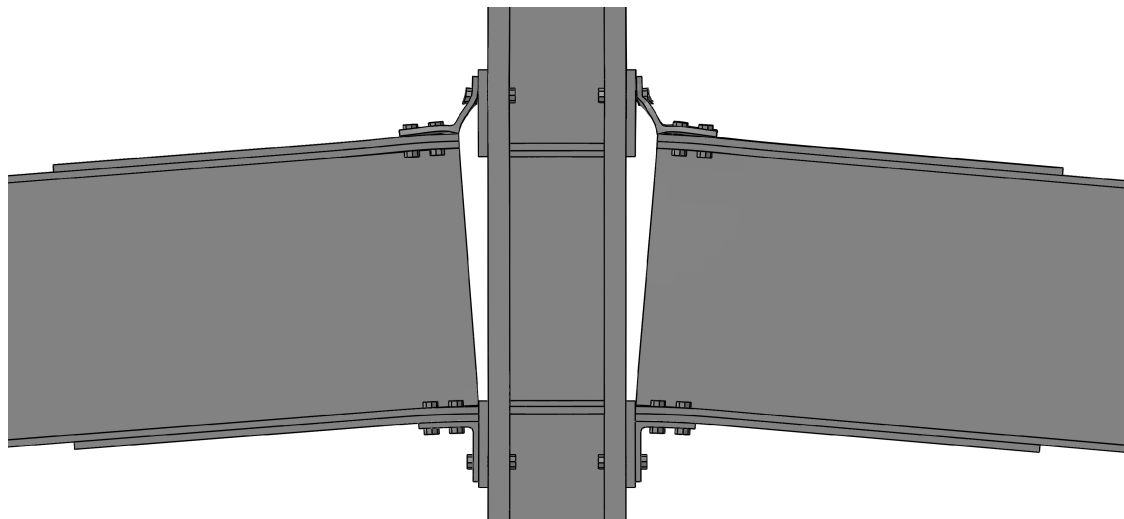


**Figure 13:  The FE model without strands at 715 degrees Celsius**

Figure 14 compares the deformed shapes of the FE models with protected strands and unprotected strands. As it is shown protecting the strands against fire have remarkably reduced the connection rotation. Whereas, applying the fire loading to the strands has led to the yielding of them which in turn results in considerable connection rotation and collapse of the structure.
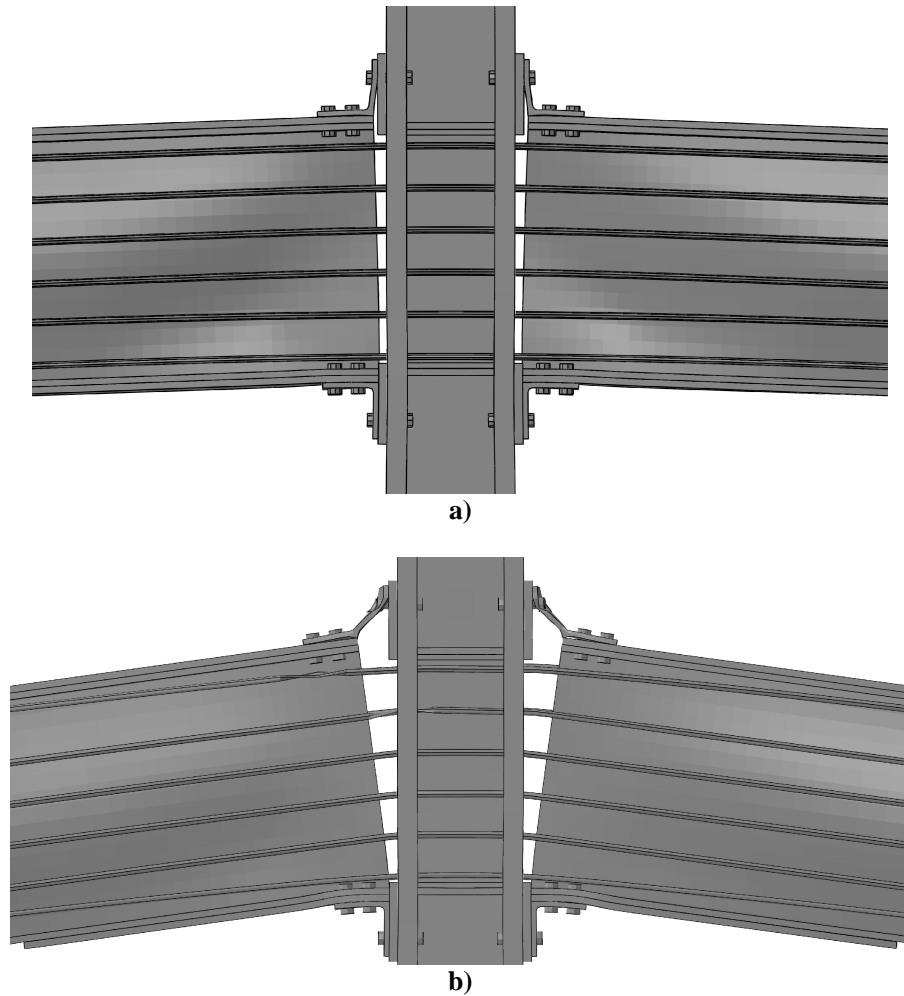
**a)**



**b)**

**Figure 14: Comparison of the FE model with strands at 723 degrees Celsius, a) protected b)
unprotected**

## 5. Conclusion

PTED connections are systems designed to be used in seismic areas to reduce the earthquake imposed damage. Since one of the most possible events during or post an earthquake is fire, evaluating the performance of a PTED connection at elevated temperatures is of great importance. An analytical study was conducted to investigate the behavior of a PTED connection with top-and-seat angles subjected to the fire loading. Three FE models with protected, unprotected and without strands were developed. The results indicate that protecting the strands against fire considerably decrease the connection rotation comparing to the other two models, and even at temperature of 750 degrees Celsius the connection does not experience extensive deformation. Therefore, using fire protection coatings for strands in a PTED connection can postpone the collapse of the structure in fire events.

The models with unprotected strands and without strands almost showed the same connection rotation. It can be concluded that when the fire loading is imposed to a PTED frame with unprotected strands, the connection does not show a much different behavior than that of a typical semi-rigid connection. Therefor unprotected strands cannot have a positive effect on improving the behavior of the PTED connection in fire scenarios.

Due to the importance of the subject, it is strongly recommended to conduct experimental researches regarding the performance of PTED connections subjected to fire scenarios and furthermore to investigate the appropriate fire protection coating materials for the posttensioning strands.

## References

[1] Christopoulos C, Filiatrault A, Uang C-M, Folz B. Posttensioned energy dissipating connections for moment-resisting steel frames. Journal of Structural Engineering, 128: 1111-20, 2002.

[2] Herning G, Garlock MM, Ricles J, Sause R, Li J. An overview of self-centering steel moment frames. Structures Congress-Don't Mess with Structural Engineers: Expanding Our Role, Austin, TX, 1412-20, 2009.

[3] Miller DK. Lessons learned from the Northridge earthquake. Engineering Structures, 20: 249-60, 1998.

[4] Tremblay R, Filiatrault A. Seismic performance of steel moment resisting frames retrofitted with a locally reduced beam section connection. Canadian Journal of Civil Engineering, 24: 78-89, 1997.

[5] Engelhardt MD, Sabol TA. Reinforcing of steel moment connections with cover plates: benefits and limitations. Engineering Structures, 20: 510-20, 1998.

[6] Garlock MM, Ricles JM, Sause R. Experimental studies of full-scale posttensioned steel connections. Journal of Structural Engineering, 131: 438-48, 2005.

[7] Ricles JM, Sause R, Garlock MM, Zhao C. Posttensioned seismic-resistant connections for steel frames. Journal of Structural Engineering, 127: 113-21, 2001.

[8] Ricles J, Sause R, Peng S, Lu L. Experimental evaluation of earthquake resistant posttensioned steel connections. Journal of Structural Engineering, 128: 850-9, 2002.

[9] Garlock MM, Ricles JM, Sause R. Cyclic load tests and analysis of bolted top-and-seat angle connections. Journal of structural Engineering, 129: 1615-25, 2003.

[10] Chou CC, Chen JH, Chen YC, Tsai KC. Evaluating performance of post-tensioned steel connections with strands and reduced flange plates. Earthquake engineering & structural dynamics, 35: 1167-85, 2006.

[11] Vasdravellis G, Karavasilis TL, Uy B. Large-scale experimental validation of steel posttensioned connections with web hourglass pins. Journal of Structural Engineering, 139: 1033-42, 2012.

[12] Jones S, Kirby P, Nethercot D. The analysis of frames with semirigid joints: A state-of-the-art report. UK: Department of Civil and Structural Engineering, University of Sheffield, 1981.

[13] Dai X, Wang Y, Bailey C. Numerical modelling of structural fire behaviour of restrained steel beam–column assemblies using typical joint types. Engineering Structures, 32: 2337-51, 2010.

[14] Yu H, Burgess I, Davison J, Plank R. Tying capacity of web cleat connections in fire, Part 1: Test and finite element simulation. Engineering Structures, 31: 651-63, 2009.

[15] Wang Y, Dai X, Bailey C. An experimental study of relative structural fire behaviour and robustness of different types of steel joint in restrained steel frames. Journal of Constructional Steel Research, 67: 1149-63, 2011.

[16] Qiang X, Bijlaard FS, Kolstein H, Jiang X. Behaviour of beam-to-column high strength steel endplate connections under fire conditions–Part 1: Experimental study. Engineering Structures, 64: 23-38, 2014.

[17] Qiang X, Bijlaard FS, Kolstein H, Jiang X. Behaviour of beam-to-column high strength steel endplate connections under fire conditions–Part 2: Numerical study. Engineering Structures, 64: 39-51, 2014.

[18] Hibbit H, Karlsson B, Sorensen E. ABAQUS User Manual, Version 6.12 ed.), Simulia,, Providence, RI, 2012.

[19] AISC 360--05, Specification for Structural Steel Buildings. American Institute of Steel Construction. Inc: Chicago, IL. ANSI A; 2005.

[20] 3: Design of steel structures–Part 1.2: General rules–Structural fire design. Brussels: European Committee for Standardization DD ENV. Eurocode E; 1993.

[21] Al-Jabri K, Seibi A, Karrech A. Modelling of unstiffened flush end-plate bolted connections in fire. Journal of Constructional Steel Research, 62: 151-9, 2006.